Liquid Crystals
Publication details, including instructions for authors and subscription information:
http://www.informaworld.com/smpp/title~content=t713926090

NMR and X-ray studies of the chromonic lyomesophases formed by some xanthone derivatives

D. Perahia[a]; E. J. Wachtel[a]; Z. Luz[a]
[a] The Weizmann Institute of Science, Rehovot, Israel

To cite this Article Perahia, D. , Wachtel, E. J. and Luz, Z.(1991) 'NMR and X-ray studies of the chromonic lyomesophases formed by some xanthone derivatives', Liquid Crystals, 9: 4, 479 — 492
To link to this Article: DOI: 10.1080/02678299108033147
URL: http://dx.doi.org/10.1080/02678299108033147

LIQUID CRYSTALS, 1991, VOL. 9, NO. 4, 479–492

NMR and X-ray studies of the chromonic lyomesophases formed by some xanthone derivatives

by D. PERAHIA, E. J. WACHTEL* and Z. LUZ
The Weizmann Institute of Science, Rehovot 76100, Israel

(*Received 4 September 1990; accepted 29 October 1990*)

Optical microscopy, NMR and X-ray measurements are presented for four chromonic lyomesogens derived from 9-xanthone. The measurements provide details about the mesogen–water binary phase diagrams of the four compounds as well as quantitative information about the ordering and structural parameters of the mesophases. All four systems exhibit peritectic phase diagrams with a nematic (N) phase at low mesogen concentration and a hexagonal (H) phase at high concentration. The results are consistent with previously suggested models for chromonic lyomesophases in which columnar aggregates are formed by stacked mesogenic molecules. In the N phase these columns are parallel to the director but are otherwise randomly distributed in the bulk solvent, while in the H phase they form a two dimensional hexagonal array.

1. Introduction

A few years ago Attwood and Lydon showed that a number of anti-allergic and anti-asthmatic drugs derived from pyrone or pyridone exhibit with water lyomesophases similar to the N and M phases of the well-known disodiumcromoglycate (DSCG)–water system [1]. These mesogenic compounds differ from the conventional lyomesophase-forming compounds (which usually consist of well-defined polar heads and flexible hydrophobic chains such as soaps and detergents) in that their molecules consist of planar aromatic moeities to which solubilizing polar groups are bonded at the periphery. Attwood and Lydon proposed [1] the term *chromonic* to describe these systems, after the DSCG–water system in which this pattern of behaviour was first identified [2–4]. More recently they discovered several more anti-asthmatic drugs and water-soluble dyes which exhibit chromonic character [5]. Other non-conventional lyotropic mesogens are known in addition to drugs or dyes, for example, polyethyleneoxy derivatives of triphenylene and tetrabenzocyclododecatetraene, salts of flufenamic and meclofenamic acids, sulfonato salts of substituted porphines as well as derivatives of guanosine and its oligomers [6–10]. Chromonic mesophases consist of columnar aggregates formed by mesogenic molecules stacked one on top of each other. In the N phase these columns retain a more or less parallel orientation but are otherwise distributed in a disordered manner in the bulk solvent, while in the more highly ordered M phase the aggregates are arranged in a two dimensional hexagonal array. To emphasize this face we shall, in the following denote the hexagonal phase by the letter H (rather than M). More recently a broader classification of possible chromonic phases, according to the stacking nature of the molecules in the columns and the symmetry of the two dimensional array of the columns, was suggested. However, several of the newly proposed structures have so far only been provisionally

* Author for correspondence

0267–8292/91 $3·00

identified [5]. A comprehensive review of the chromonic mesophases as well as an article providing further insight into these mesophases have recently been published [11, 12].

The characterization of the mesomorphic properties of the new drugs and water-soluble dyes by Attwood and Lydon was made predominantly by optical microscopy and miscibility studies, and to a lesser extent also by X-ray diffraction [1, 5]. While these observations provide sufficient information to allow their classification, they do not provide quantitative data about the range of stability of the various phases and about their internal structure. In the present work we attempt to fill in this gap and present results of NMR and X-ray measurements on the mesophases of four of the drug compounds described in reference [1]. They all are derivatives of 9-xanthone

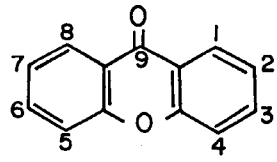

and are thus related to DSCG in that they all have in common the benzpyrene (chromone) moiety. The compounds studied are listed in table 1, where their short-hand symbols are those given by the manufacturing companies, Roussel Ltd. (Ru and Glaxo Ltd. (AH), but we shall refer to them as systems I to IV as indicated in the first column of the table. The NMR measurements involve predominantly the deuterium signal of the solvent D_2O, which is used to establish the binary phase diagrams of the various compounds with water. Some additional measurements on the water ^{17}O, the counter ions ^{23}Na and the mesogen ^{13}C signals provided further information on the ordering characteristics of the mesophases, while the X-ray measurements confirmed the assignment and also provided quantitative information on the dimensions of the relevant structural parameters.

2. Experimental

The mesogenic compounds were kindly provided by Roussel Ltd. (Ru 31156) and Glaxo Ltd. (AH 7079, AH 6556, AH 7725) and were used without further treatment. Solutions were prepared gravimetrically in D_2O (>99 at%) for all NMR measurements and in H_2O for the X-ray and optical microscopy studies. Oxygen-17 measurements were made with water enriched to 5 at% ^{17}O. The concentrations of the solutions are given in wt%, i.e.

$$100 \times (\text{weight of mesogen})/(\text{weight of solvent water} + \text{weight of mesogen}).$$

The optical microscopy, NMR and X-ray measurements were performed as described in previous publications from this laboratory [4].

Table 1. The 9-xanthone derivatives used in the present study.

	Common name	R_2	R_5	R_7	Cation
I	Ru 31156	COO^-	n-C_6H_{13}	$S(O)(CH_3)NH$	$Tris^+$‡
II	AH 7079	N_4^-†	H	OCH_3	Na^+
III	AH 6556	COO^-	H	OCH_3	Na^+
IV	AH 7725	COO^-	H	$O(CH_2)_2OH$	Na^+

† 2-Tetrazole.
‡ $^+H_3NC(CH_2OH)_3$.

3. Results and discussion

3.1. *Optical microscopy and NMR*

Figure 1 shows optical micrographs of contact preparations of the four xanthone–water systems studied. As may be seen, all compounds exhibit, with increasing water concentration, the expected transformations from solid via the H and N phases to the isotropic liquid [1]. The N phase exhibits schlieren textures characteristic of nematic phases, while the textures of the hexagonal H phases are generally ill-defined and appear grainy or, in some cases, rippled. The boundaries between the isotropic (I), nematic, hexagonal and solid (S) phase are, however, well defined and confirm the phase sequence first described by Attwood and Lydon [1].

In figure 2 we summarize the water–mesogen binary phase diagrams of the compounds studied. These were predominantly constructed from deuterium NMR measurements on several series of binary mixtures in D_2O and, for system I, also by optical microscopy. The latter were performed on samples enclosed in sealed

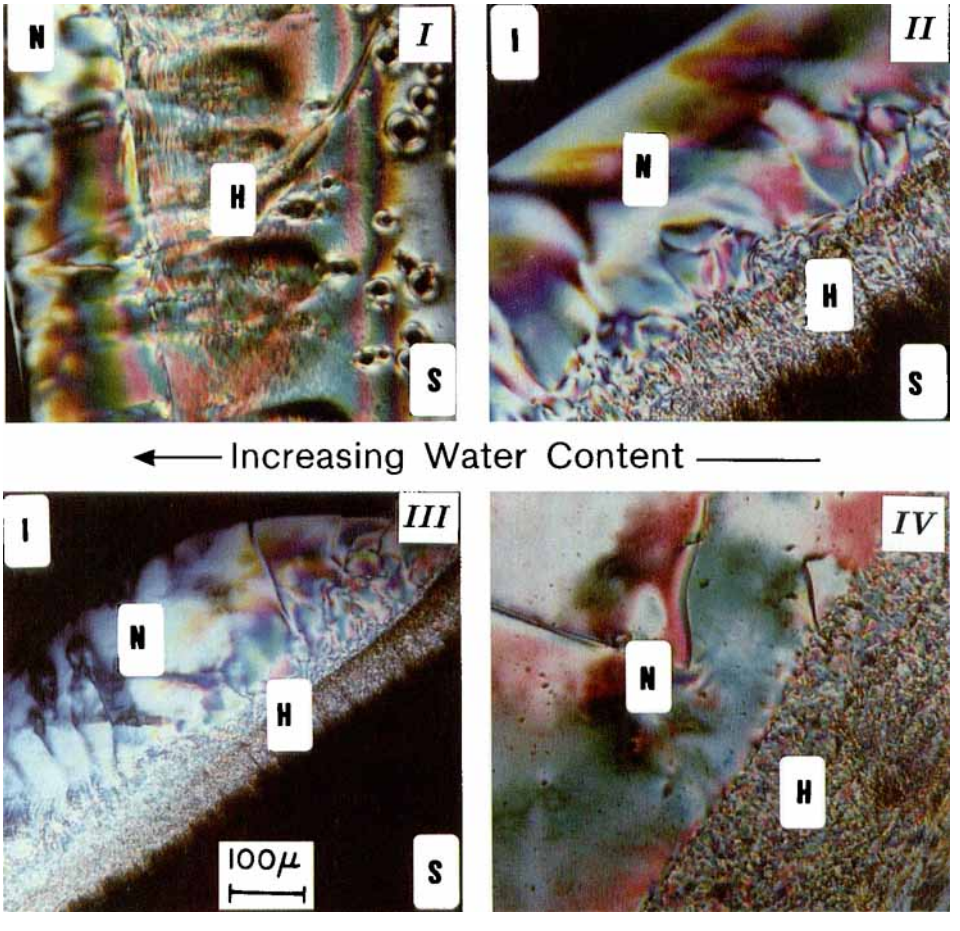

Figure 1. Polarizing optical microscope pictures of contact preparations formed from the four xanthone derivatives studied in the present work, with water. In all cases, the water concentration decreases from left to right. The labels I to IV refer to the different compounds as defined in table 1.

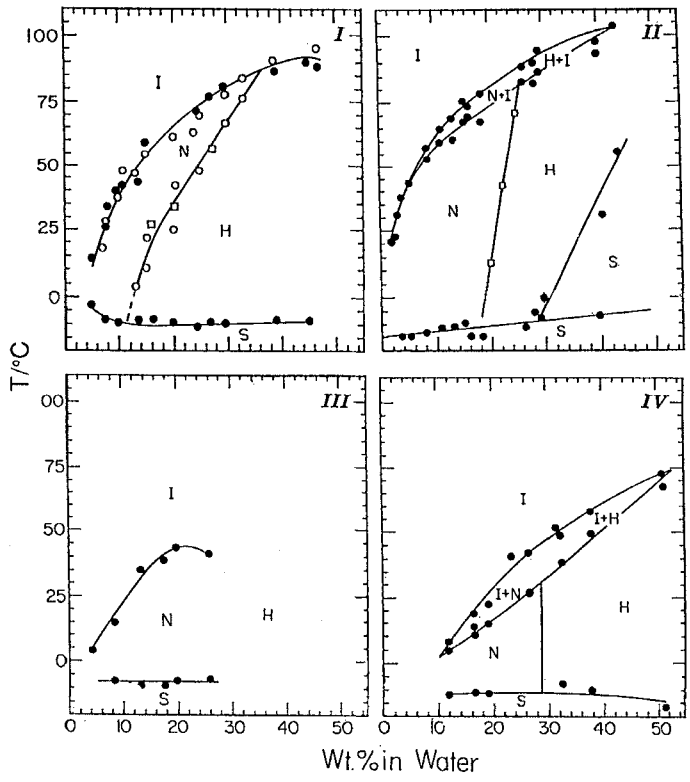

Figure 2. Binary phase diagrams of the four mesogenic systems studied with water. The solid circles, open circles and open squares are experimental points determined as described in the text by deuterium NMR, optical microscopy and X-ray, respectively.

rectangular glass tubes ($2 \times 0{\cdot}1$ mm) containing the desired solution in H_2O. The transitions involving the isotropic, nematic and hexagonal phases, as well as the extent of the biphasic regions could readily be identified by this method and the results obtained are indicated by open circles. The liquidus and solidus curves of the I to N and I to H transitions as obtained by NMR are indicated by full circles. They were determined, respectively, from the first appearance of a doublet in the deuterium spectrum upon cooling the solution within the NMR spectrometer, and from the lowest temperatures at which the singlet due to the isotropic liquid was still observed. The transition from the mesophase to solid was recognized by the sudden broadening of the NMR signal. Sometimes, for example in system II, this broadening occurred in two steps, suggesting additional transformations between different solid phases. The transition temperatures determined by the NMR measurements are indicated in figure 2 by solid circles.

In all of the systems studied, a well-resolved doublet was observed in the deuterium spectrum, when the samples were cooled into the mesophase region, within the NMR spectrometer, indicating that, under these conditions, the domains are well-aligned, with the director orienting either parallel to or in a plane perpendicular to, the magnetic field direction. Sample rotation experiments [4] with the H phase and with the N phase at low temperatures showed that in all cases, the mesophases are uniaxial and the

director aligns perpendicular to the field direction. This corresponds to a negative anisotropic magnetic susceptibility ($\Delta\chi = \chi_{\parallel} - \chi_{\perp} < 0$), as was also found in the N and H phases of the DSCG–water system [4].

The observed full splitting, ν_Q^D of the D_2O deuterium spectrum in different solutions of the four compounds studied as a function of temperature are summarized in figure 3. Since the domains are aligned perpendicular to the field direction, this splitting gives directly the principal component of the average quadrupole interaction of the water deuterons in the mesophase. Examples of spectra of solutions of I at two different concentrations are shown in figure 4. For this compound in solutions containing 20 to 40 wt %, the splitting was found to vanish at certain temperatures and we interpret this behaviour as due to a change in sign of the quadrupole interaction parameter [4]. Otherwise the behaviour of all of the systems is quite similar in that the magnitude of the quadrupole splitting increases with concentration and decreases with temperature. The splitting in the mesophases of system III is exceptionally small as is also the overall range of stability of its mesomorphic state.

The ^{17}O quadrupole splitting ν_Q^O in solutions containing water enriched with oxygen-17 exhibited a similar behaviour to that of the deuterons. Results obtained

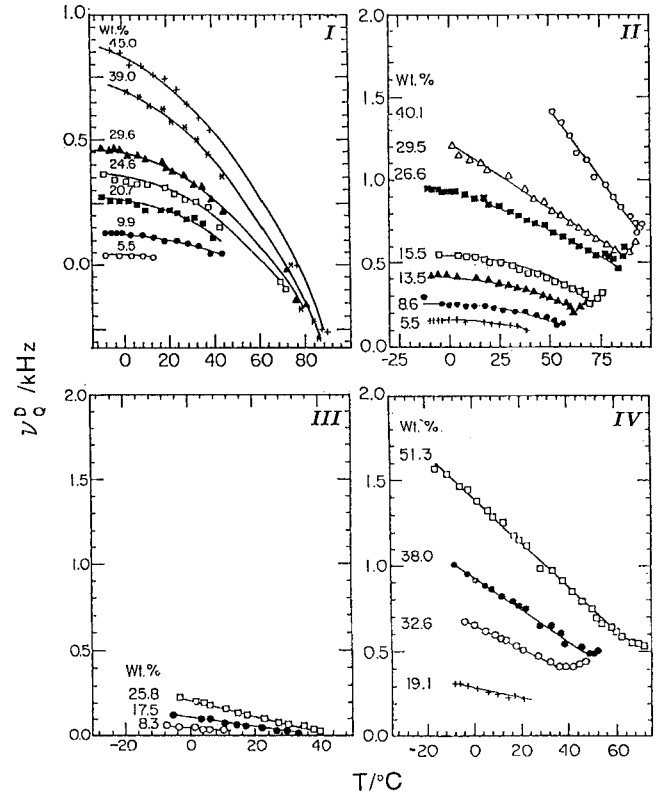

Figure 3. The temperature dependence of the average quadrupole interaction of the water deuterons, as measured from the full splitting of the deuterium NMR spectra obtained by slow cooling within the magnetic field of different solutions of the four systems studied. It is assumed that the sign of the interaction is positive except for some regions in the phase diagram of I, where apparently a sign change takes place.

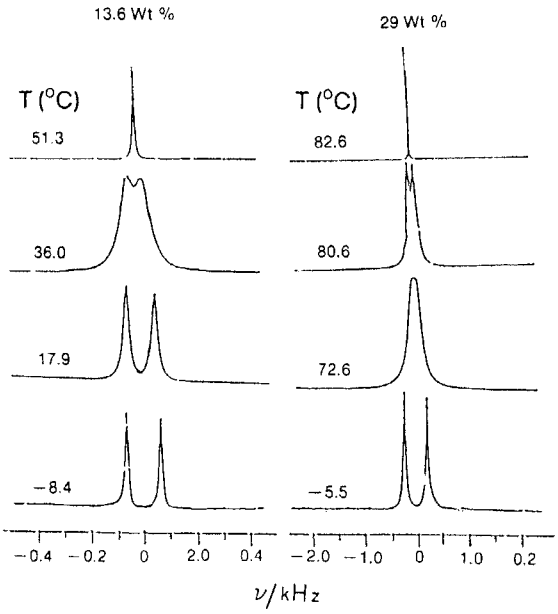

Figure 4. Deuterium NMR spectra at 46·07 MHz in two D_2O solutions of I at different temperatures. The measurements were made on samples which were aligned by slow cooling of the isotropic liquid to the indicated temperatures within the magnetic field of the NMR spectrometer.

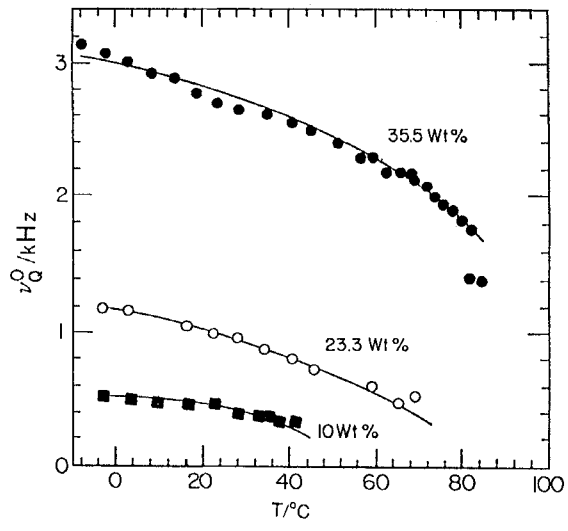

Figure 5. The average quadrupole interaction of the water ^{17}O nuclei (assumed to be positive) in the mesophase region of three solutions of I. The measurements were made in solutions containing water enriched to 5 at% oxygen-17.

from three solutions of system I are shown in figure 5. These results, together with those for the deuterons have been used to estimate the order parameters for the water solvent in the mesophase region. Values ranging from 5×10^{-3} to 8×10^{-3} for $|S_{xx} - S_{yy}|$ and 0·01 to 0·10 for $|S_{zz}|$ were obtained. These are in the same range as those obtained for the DSCG mesophases [4].

We have also recorded the ^{23}Na NMR spectra in the three systems II, III and IV, where the counterions are sodium. The measured quadrupole splitting, ν_Q^{Na} are shown in figure 6. Note that for concentrated solutions and high temperatures (and also for the intermediate-concentration solutions) a negative sign for ν_Q^{Na} was assumed, so that similar trends for the sodium splitting in all solutions are obtained. The assumption that ν_Q^{Na} is positive in the rest of the solutions is, of course, arbitrary. Unlike the ^{17}O and D of the solvent water, the splittings of the ^{23}Na are much less dependent on the mesogen concentration. We note in particular, that for system II, identical ν_Q^{Na}s are obtained for solutions with 9·3, 18·7 and 40·1 wt % mesogen over the whole temperature range of the mesophase. These results can be explained by assuming that most of the sodium is associated with the columns and only very few ions are free in the bulk. The sodium splitting then reflects the ordering of the micelles which apparently is not concentration dependent (between 9 and 40 wt %), but decreases very significantly with increasing temperature.

Additional NMR observations were made on the ^{13}C signal of a 30 wt % solution of system I. In the isotropic phase this solution exhibits, in addition to many other peaks, three isolated sharp signals in the low field region of the spectrum ($\sigma > 150$ ppm) at $\sigma^a = 157{\cdot}93$, $\sigma^b = 172{\cdot}03$ and $\sigma^c = 177{\cdot}50$ ppm (see the upper trace in figure 7). On the basis of ^{13}C chemical shift data [13], we identify these peaks with (*a*) the tertiary carbons next to the oxygen in the pyrone ring, (*b*) the carboxyl carbon, and (*c*) the carbonyl carbon. When the temperature is lowered to 78°C, which is just below the clearing temperature of the solution, the spectral lines shift and broaden quite considerably, with some of the peaks completely disappearing in the noise (see the

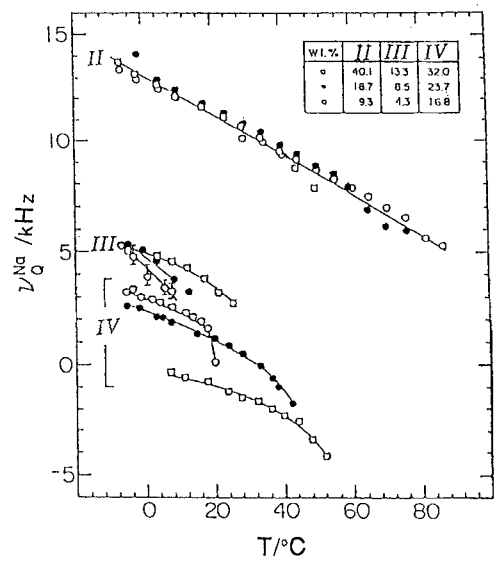

Figure 6. The ^{23}Na average quadrupole splitting in solutions of II, III and IV. ν_Q^{Na} is assumed to be positive except for certain ranges of system IV.

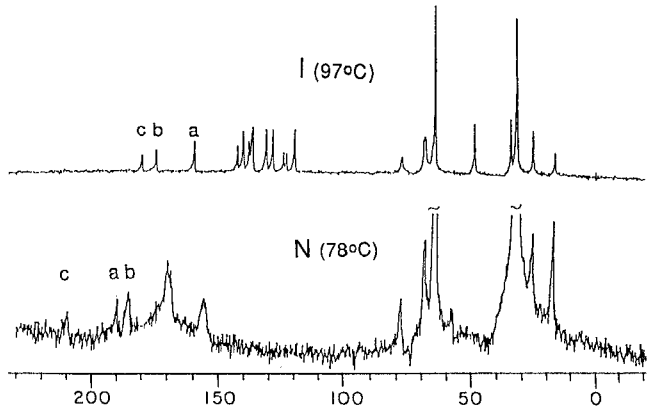

Figure 7. Carbon-13 NMR spectra at 75·45 MHz of a 30 wt% solution of I in the liquid and mesophase regions at the temperatures indicated.

lower trace in figure 7). The three low-field peaks are also shifted but remain relatively sharp; they appear at 205·5, 186 and 184 ppm. Their identification in the mesophase spectrum with carbons *a*, *b* and *c* is however more subtle. If we assume that the pyrone carbons *a* and *c* undergo similar shifts at the isotropic to nematic transition we can identify the 205·5 and 186 ppm peaks with carbon *c* and *a* and the 184 ppm peak with the carboxyl carbon, i.e. the pyrone carbons undergo a down-field shift of about 28 ppm while the carboxyl carbon shifts by 12 ppm. Assuming that the rigid aromatic moieties of the mesogen molecules are on average distributed in a plane perpendicular to the long axis of the micelles and recalling that the sample aligns with the director perpendicular to the magnetic field direction, we can estimate the orientational order parameter, S of the micellar columns in the mesophase from [14]

$$S = 3\frac{\sigma_i - \sigma_{LC}}{\Delta\sigma}. \tag{1}$$

Here σ_{LC} and σ_i are the chemical shifts observed in the mesophase and isotropic liquid respectively, $\Delta\sigma = \sigma_{11} - (\sigma_{22} + \sigma_{33})/2$, where σ_{11} is the static ^{13}C chemical of the aromatic carbons perpendicular to the aromatic plane and σ_{22}, σ_{33} the corresponding values within the plane. From ^{13}C chemical shift tables [15] we estimate $\Delta\sigma$ for the aromatic carbons to be about -150 ppm giving $S \approx 0{\cdot}56$. A similar calculation for the carboxylate carbon using $\Delta\sigma = -100$ ppm gives $S = 0{\cdot}36$. The lower value obtained for the latter carbon is most likely due to the fact that the carboxylic group is not strictly coplanar with the aromatic plane, but rather undergoes restricted reorientations about its C–C bond. We believe therefore that the value derived from the aromatic carbons is more realistic. It would be interesting to extend these measurements to a wide range of concentrations and temperatures but the sensitivity of our spectrometer was not sufficient for such extensive measurements to be carried out.

None of the NMR spectral data exhibited any discontinuity in either the quadrupole splitting or in the width of the multiplet components, that could be associated with the N to H transition and therefore the corresponding equilibrium lines in the phase diagram could not be obtained from these measurements. For most systems this information could, however, be derived from optical microscopy as described previously and from the X-ray measurements explained in the next section.

3.2. *X-ray diffraction measurements*

X-ray diffraction measurements were made on solutions of all of the systems studied in both the low and high angle regions. These measurements provided structural parameters relevant to the N and H phases and were particularly useful in determining the equilibrium line between these phases because of their different diffraction patterns. Figure 8 illustrates this difference in the one dimensional X-ray profiles for three solutions of I with concentrations of 10·0, 27·4, and 40·0 wt%. These solutions correspond to samples exhibiting respectively only N, both N and H, and only H phases (see phase diagram I in figure 2). In the low concentration solution, only a single, relatively broad peak at around $\Theta \approx 0{\cdot}5^\circ$ is observed. This peak may be identified with scattering due to positional correlations of the columnar aggregates in the N phase and the corresponding d spacing (~ 88 Å) is therefore related to the average distance between columns in this phase.

Some information on the ordering characteristic of the aggregates in the mesomorphic state can be obtained from the widths Δ, of the diffraction peaks with is given approximately by the quadrature sum [6]

$$\Delta(2\Theta) = \lambda\left[\left(\frac{1}{Nd}\right)^2 + \left(\frac{h^2\pi^2\delta^2}{2d^3}\right)^2\right]^{1/2}, \tag{2}$$

where λ is the X-ray wavelength (1·54 Å in this case), h is the order of the diffraction, N is the number of repeats d in the lattice and δ is the half width of an assumed gaussian distribution in the parameter, d. The width $\Delta(2\Theta)$ is thus a sum of two contributions, the

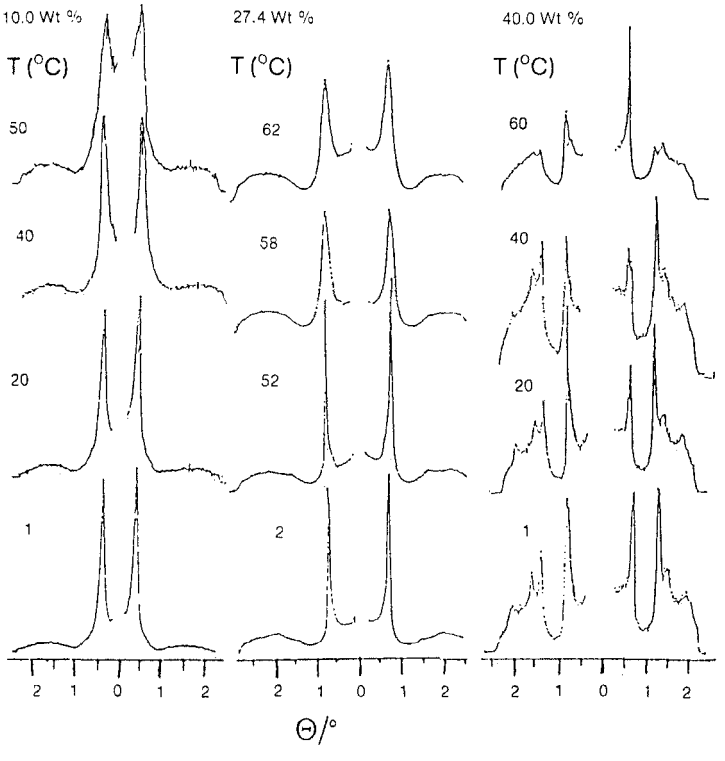

Figure 8. One dimensional X-ray diffraction patterns from three solutions of I at several temperatures.

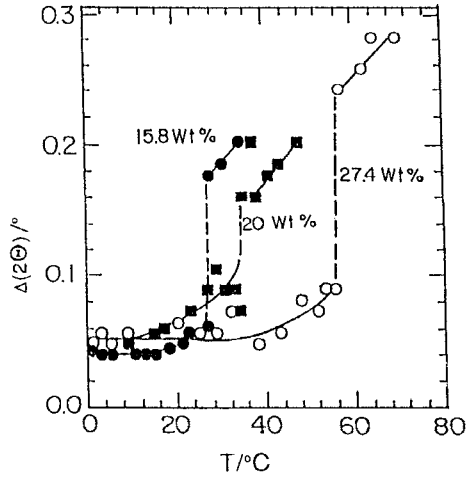

Figure 9. Plots of the linewidth of the first X-ray diffraction peak in different solutions of I as a function of temperature within the mesophase region.

finite size Nd of the array (the first term in equation (2)) and the disorder in the repeat units (the second term). Assuming that in the nematic phase the latter term is the main source for the linewidth, yields $\delta \approx 18$ Å where we have used $h = 1$ and the experimental value for the 10 wt% solution, $\Delta(2\Theta) = 0{\cdot}21°$. The results for d and δ are almost independent of temperature within the mesophase phase but, as would be expected, they depend quite significantly on the concentration of the solutions.

The low angle X-ray pattern observed in the H phase is quite different from that of the nematic phase. This is clearly demonstrated in the diffraction patterns shown in the right hand column of figure 8, which corresponds to a solution that exhibits only the H phase. They show a relatively strong and sharp inner peak and usually two to three additional weaker peaks. Their d spacings can be indexed on a two dimensional hexagonal lattice with the sequence of peaks corresponding to the $\{1,0\}$, $\{1,1\}$, $\{2,0\}$ and $\{2,1\}$ reflections in the ratio of $1:1/\sqrt{3}:1/2:1/\sqrt{7}$. The sharpness of these reflections and the fact that as many as four of them can be observed indicate that the H phase is quite well-ordered. Referring again to equation (2), the fact that the linewidth does not appear to increase from the $\{1,0\}$ to the $\{2,0\}$ reflection strongly suggests that in the H phase the first term is dominant. This allows us to estimate a lower bound for the lateral coherence length, Nd, of the hexagonal array. For example, for the 40 wt% sample of I, $Nd_{10} \approx 1800$ Å. As for the N phase, the d spacings are relatively independent of temperature but change with the concentration of the mesogen.

The distinction between the X-ray patterns in the N and H phases is well demonstrated by the results for the 27·4 wt% solution (see the middle column in figure 7). This solution undergoes a transition from H to N at about 55°C (see the phase diagram I in figure 2). As may be seen at all temperatures this solution exhibits a dominant inner peak at approximately the same scattering angle $\Theta \sim 0{\cdot}76°$ ($d = 55$ Å) but the width of this reflection below 55°C is considerably less than above this temperature. In fact, a plot of the peak width as a function of temperature shows a discontinuity at 55°C (see figure 9) which we associate with the H to N transition. This is further supported by the fact that X-ray profiles taken below 55°C also exhibit two (quite weak) additional diffraction peaks with spacings $d/\sqrt{3}$ and $d/2$ as expected for a

hexagonal array. The width of the inner diffraction peak may thus serve to distinguish between the N and H phases and to determine the equilibrium line between them in binary phase diagrams. Thus in the phase diagram of II the N to H boundary line is somewhat inclined and therefore as for I, the transition could be observed from the temperature dependence of the width of the diffraction peak in the appropriate concentration range (see diagram II of figure 2). In solutions of IV the N/H boundary is almost exactly vertical and therefore no solution was found which exhibited a discontinuity in the width of the diffraction peak as a function of temperature. However, all solutions below 28 wt% showed only a single broad diffraction peak, characteristic of the nematic phase while above this concentration a single narrow inner peak may be seen, fixing the N/H equilibrium line as shown in diagram IV of figure 2. Contact preparations indicate that the H phase exists also in solutions of III (see figure 1). However, in the concentration range that we have used (up to 28 wt%) no transition from N to H could be detected by X-ray (or by NMR).

In contrast to the discontinuity in the width of the inner diffraction peak on going from N to H, its position does not seem to be affected by this transition. This is demonstrated in figure 10 where a plot of the *d* spacing of the inner diffraction is plotted as a function of temperature for several solutions of I and in table 2, where additional data on solutions of compounds II, III and IV are given. In all cases, no discontinuity in *d* is observed as the N/H boundary line is crossed. We may thus view the N to H transition as a continuous transformation resulting from the increase in the rod concentration. When this concentration exceeds a certain critical value the positional fluctuations characterizing the N phase diminish and the system acquires a hexagonal order. This lateral ordering becomes continuously more pronounced with increasing concentration as reflected in the increase in intensity of the higher order reflections.

In the X-ray profiles of both the N and H phases an additional broad feature at $\Theta \approx 13{\cdot}1°$ corresponding to 3·4 Å is also found. It is superimposed upon the very diffuse scattering from the solvent water. The 3·4 Å peak is ascribed to the stacking distance of

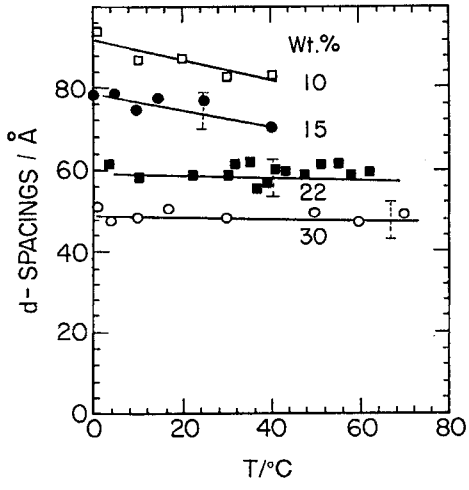

Figure 10. Plots of the first X-ray diffraction maximum observed in several solutions of I as function of temperature. The vertical bars indicate the H to N transition temperature for the various solutions.

Table 2. *d* spacing of the innermost diffraction peak in several solutions of compounds II, III and IV at different temperatures, *T* and concentrations.

II				III				IV			
12·0 wt %		23·0 wt %		16·9 wt %		26·7 wt %		20·0 wt %		38·9 wt %	
T/°C	*d*/Å	*T*/°C	*d*/Å	*T*/°C	*d*/Å	*T*/°C	*d*/Å	*T*/°C	*d*/Å	*T*/°C	*d*/Å
0	52·0	0	41·5	0	38·0	0	32·0	0	41·2	2	26·3
10	52·1	10	40·9	13	36·5	14	31·6	3	42·1	10	26·4
27	50·1	27	40·7	25	36·5	22	31·6	18	39·0	29	26·7
40	52·0	40	41·4	28	37·5	32	31·2	30	39·0	40	25·4
50	50·1	50	41·7	32	36·4	42	31·9			45	24·1
65	53·0	60	41·2	37	36·4	52	32·7			60	23·4

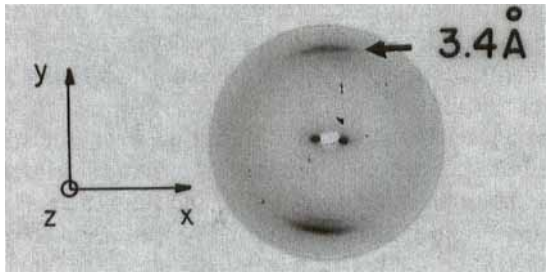

Figure 11. X-ray photograph of a 30 wt % sample of I in phase H (at 0°C) after alignment in a 21 kG magnetic field. The X-ray beam was along *z* while the capillary containing the sample was parallel to the *y* axis. The magnetic field was along *x*. Note the weak meridional reflection next to the 3·4 Å arcs due to the K_β component of the X-ray beam.

the rigid xanthone moieties within the columns. This is well demonstrated in the X-ray pattern obtained from a magnetically aligned sample. In figure 11 is shown an X-ray photograph of a 30 wt % sample of I in the H phase (at 0°C) which was prealigned in a magnetic field of 21 kG. The alignment was affected by allowing the sample to cool within the magnetic field from the isotropic through the nematic to the H phase. The magnetic field (*x*) was perpendicular to the capillary (*y*) axis and the photograph was taken with an X-ray beam along the *z* direction. The photograph shows two sets of reflections; one at low angles along the horizontal (*x*) axis due to lateral packing of the columns and a second along the meridian (*y*) axis at 3·4 Å, reflecting the stacking repeat distance within the columns. The fact that the two sets of reflections are orthogonal is consistent with the columnar structure assumed for these phases and their orientation on the X-ray photograph is as expected from the negative anisotropic magnetic susceptibility determined by the NMR experiments.

The linewidth of the 3·4 Å peak is quite similar in the N and H phases and is of the order of 1·6° for the four systems studied. Referring to equation (2) it is difficult to ascertain which of the two terms is more important in determining $\Delta(2\Theta)$. If we assume that the stacking is well ordered, then an average length of columns of $Nd \sim 54$ Å can be inferred from the observed peak width.

4. Summary and conclusions

The results obtained for the four chromonic systems studied in the present work are similar to those obtained for the prototype system of this family of lyotropics, i.e. the DSCG–water system. It appears that in all cases the structural units consist of columnar aggregates formed by the stacking of the mesogenic molecules parallel to each other. Beyond a certain critical concentration at room temperature and below, spontaneous orientational ordering sets in, resulting in the nematic phase. The transition to the hexagonal phase apparently occurs once a second critical concentration of aggregates has been reached. The intramolecular stacking order appears to be unchanged across the phase boundary. This second transformation could well correspond to a continuous transition. This view is supported by other evidence; so far, no DSC peaks have been observed in the N to H transitions of chromonic liquid crystals and in some cases, the hexagonal phase is formed directly from the isotropic liquid (e.g. compound IV at high temperatures).

The characteristic packing distances measured for the different compounds are similar for similar molar concentrations of mesogen. In all cases, however, these distances are large when compared to the expected lateral dimensions of the molecules. Calculating the volume of the water with respect to the volume occupied by the mesogen, and comparing the sum with the volume of the unit cell derived from the X-ray data, leads to the conclusion that the asymmetric unit of the structure consists of two molecules. This would be consistent with a model for the mesophases involving dimers.

We are grateful to Roussel Ltd. for providing the Ru 31156 sample and to Glaxo Ltd. for the AH 7079, AH 6556 and AH 7725.

References

[1] ATTWOOD, T. K., and LYDON, J. E., 1984, *Molec. Crystals liq. Crystals*, **108**, 349.

[2] COX, J. S. G., WOODARD, G. D., and MCCRONE, W. C., 1971, *J. Pharm. Sci.*, **60**, 1458. HARTSHORNE, N. H., and WOODARD, G. D., 1973, *Molec. Crystals liq. Crystals*, **23**, 343; *Ibid.*, **64**, 153.

[3] LYDON, J. E., 1980, *Molec. Crystals liq. Crystals*, **64**, 19. ATTWOOD, T. K., and LYDON, J. E., 1986, *Molec. Crystals liq. Crystals*, **4**, 9.

[4] GOLDFARB, D., LABES, M. M., LUZ, Z., and POUPKO, R., 1982, *Molec. Crystals liq. Crystals*, **87**, 259. GOLDFARB, D., MOSELEY, M. E., LABES, M. M., and LUZ, Z., 1982, *Molec. Crystals liq. Crystals*, **89**, 119. PERAHIA, D., GOLDFARB, D., and LUZ, Z., 1984, *Molec. Crystals liq. Crystals*, **108**, 107. GOLDFARB, D., LUZ, Z., SPIELBERG, N., and ZIMMERMANN, H., 1985, *Molec. Crystals liq. Crystals*, **126**, 225. PERAHIA, D., LUZ, Z., WACHTEL, E. J., and ZIMMERMANN, H., 1987, *Liq. Crystals*, **2**, 473.

[5] ATTWOOD, T. K., LYDON, J. E., and JONES, F., 1986, *Liq. Crystals*, **1**, 499. TURNER, J. E., and LYDON, J. E., 1988, *Molec. Crystals liq. Crystals*, **5**, 93. SADLER, D. E., SHANNON, M. D., TOLLIN, P., YOUNG, D. W., EDMONDSON, M., and RAINSFORD, P., 1986, *Liq Crystals*, **1**, 509.

[6] SCHWARTZ, S., CAIN, J. E., DRATZ, E. A., and BLASIE, J. K., 1975, *Biophysical J.*, **15**, 1201. CORNE, S. A., HOLMES, M. C., JACKSON, P. H., PARKER, D., and JOLLEY, K. W., 1986, *J. Phys., Paris*, **47**, 2135.

[7] ZIMMERMANN, Z., POUPKO, R., LUZ, Z., and BILLARD, J., 1989, *Liq Crystals*, **6**, 151.

[8] ECKERT, T., and FISCHER, W., 1981, *Colloid Polym. Sci.*, **259**, 553. FISCHER, W., and ECKERT, T., 1982, *Colloid Polym. Sci.*, **260**, 880. KUSTANOVICH, I., POUPKO, R., ZIMMERMANN, H., LUZ, Z., and LABES, M. M., 1985, *J. Am. chem. Soc.*, **107**, 3494.

[9] KUSMA, M. R., SKARDA, V., and LABES, M. M., 1984, *J. chem. Phys.*, **81**, 2925.

[10] SPADA, G. P., CARCURO, A., COLONNA, F. P., GARBESI, A., and GOTTARELLI, G., 1988, *Liq. Crystals*, **3**, 651. MARIANI, P., MAZABARD, C., GARBESI, A., and SPADA, G. P., 1989, *J. Am. chem. Soc.*, **111**, 6369. BONAZZI, S., GARBESI, A., GOTTARELLI, G., MARIANI, P., and SPADA, G. P., 1990, *The 13th International Liquid Crystal Conference*, 22–27 July 1990, University of British Columbia, Canada, Book I, p. 126.

[11] VASILEVSKAYA, A. S., GENERALOVA, E. V., and SONIN, A. S., 1989, *Usp. Khim.*, **58**, 1575.

[12] ATTWOOD, T. K., LYDON, J. E., HALL, C., and TIDDY, G. J. T., 1990, *Liq. Crystals*, **7**, 657.

[13] BREITMEIER, E., HAAS, G., and VOELTER, W., 1979, *Atlas of Carbon-13 NMR Data*, Vol. 2, (Heyden) (see, for example, compounds 1934 and 2307).

[14] EMSLEY, J. W., and LINDEN, J. C., 1975, *NMR Spectroscopy Using Liquid Crystal Solvents* (Pergamon Press), Chap. 8.

[15] DUNCAN, T. M., 1987, *J. Phys. Chem. Ref. Data*, **16**, 125. VEEMAN, W. S., 1984, *Prog. NMR Spectrosc.*, **16**, 193. FYFE, C. A., 1983, *Solid State NMR for Chemists* (C.R.C. Press), Chap. 5.